RAIRO-Theor. Inf. Appl. **42** (2008) 21–36
DOI: 10.1051/ita:2007045

Available online at:
www.rairo-ita.org

ABOUT THE DOMINO PROBLEM IN THE HYPERBOLIC PLANE FROM AN ALGORITHMIC POINT OF VIEW *

Maurice Margenstern[1]

Abstract. This paper is a contribution to the general tiling problem for the hyperbolic plane. It is an intermediary result between the result obtained by R. Robinson [*Invent. Math.* **44** (1978) 259–264] and the conjecture that the problem is undecidable.

Mathematics Subject Classification. 52C20, 05B45.

Introduction

The question, whether it is possible to tile the plane with copies of a fixed set of tiles was raised by Wang [11] in the late 50's of the previous century. Wang solved the *partial* problem which consists in fixing an initial finite set of tiles: indeed, fixing one tile is enough to entail the undecidability of the problem. The general case, when no initial tile is fixed, was proved undecidable by Berger in 1966 [1]. Both Wang's and Berger's proofs deal with the problem in the Euclidean plane. In 1971, Robinson found an alternative proof of the undecidability of the general problem in the Euclidean plane, see [9]. In this 1971 paper, he raises the question of the general problem for the hyperbolic plane. Seven years later, in 1978, he proved that in the hyperbolic plane, the partial problem is undecidable, see [10]. Up to now, the general problem is still open in the hyperbolic plane.

In this paper, we sketch a proof that a generalized origin-constrained problem is also undecidable in the hyperbolic plane.

The **generalized origin-constrained problem** is defined as follows. Consider a given set of prototiles T. Say that a set Ω of prototiles with $\Omega \subseteq T$ is a set of

Keywords and phrases. Tilings, tiling problem, hyperbolic plane, origin-constrained problem.

* *This paper is dedicated to my old friend Serge Grigorieff, at the occasion of his sixtieth birthday.*

[1] Université Paul Verlaine - Metz, IUT de Metz; margens@univ-metz.fr

generalized origins, and its elements are simply called **origins**, if and only if:

(i) There is a positive number k such that in the ball of radius k around any origin ω, there are at least two origins ω_1 and ω_2 with ω, ω_1 and ω_2 not on the same line.

(ii) There are infinitely many rays each one containing infinitely many origins.

The generalized origin-constrained problem consists in finding whether there is an algorithm which, for any finite set of prototiles T selects a subset Ω such that there is a tiling consisting of copies of T which satisfies properties (i) and (ii) with respect to Ω.

It turns out that, in the Euclidean plane, the proofs which we have of the undecidability of the tiling problem with no restriction, also satisfy properties (i) and (ii) with respect to the set of origins in the given set of tiles.

In this paper, we prove that the generalized origin-constrained problem is undecidable in the hyperbolic plane.

1. The tiling $\{7, 3\}$ and the mantilla

Within the short room of this paper, it is not possible to give an introduction to hyperbolic geometry. It is also not possible to introduce the tools which are used in the paper in order to locate the tiles in the considered tiling. For both introductions, we refer the reader to [8] where the tools are described with full details. In this book, there is also a substantial introduction to hyperbolic geometry. Also there, the reader will find a precise description of Poincaré's disc model which is intensively used in [8], as well as in this paper.

1.1. The tiling $\{7, 3\}$

The tiling $\{7, 3\}$ is a particular case in the infinite family of tilings of the hyperbolic plane denoted by $\{p, q\}$. The tiling $\{p, q\}$ is generated from a regular polygon with p sides and an interior angle $\frac{2\pi}{q}$ by reflection of the polygon in its edges and, recursively, of the images in their edges. The tiling $\{7, 3\}$ corresponds to the case when $p = 7$ and $q = 3$. For this reason, we shall call it the **ternary heptagrid**, for short, **heptagrid**.

The ternary heptagrid is illustrated by the left-hand side picture of Figure 1.

On the right-hand side of the same figure, the picture illustrates a situation which will be intensively used in this paper. We can see two rays which delimit a region with coloured tiles. A reader, familiar with [8], will recognize a Fibonacci tree in the set of tiles defined in this way. From [8] and [3], we know that the Fibonacci tree defines a bijection with this set of tiles. It also gives an efficient way to locate the tiles of this set. At last, displaying seven Fibonacci trees around a fixed tile allows to exactly cover the ternary heptagrid with no overlapping of tiles.

Now, note that the rays which delimit the considered set of tiles, we call this an **angular sector**, have a particular property. The supporting lines pass through the

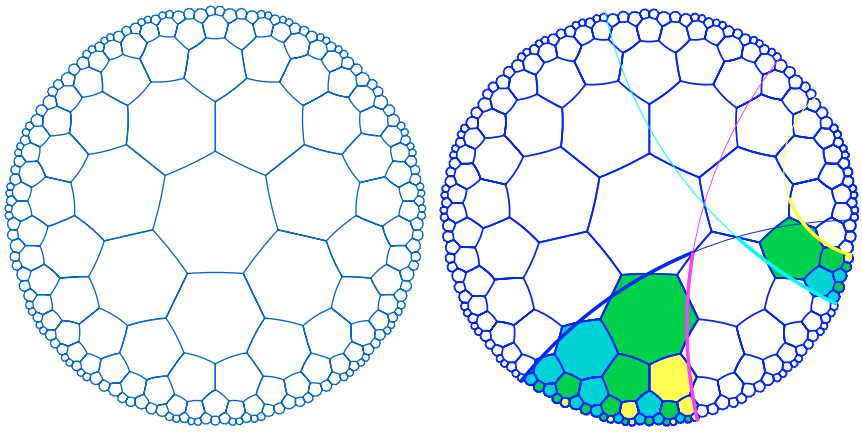

FIGURE 1. To the left: a representation of the ternary heptagrid in the Poncaré's disc model of the hyperbolic plane. To the right: the definition of the mid-point lines and the sector which delimits a Fibonacci tree.

mid-points of edges of the tiling. More precisely, the mid-points of two consecutive edges of a tile uniquely define such a line which we call a **mid-point line**.

1.2. The mantilla

Now, let us introduce the mantilla, which is the basis of the construction which we need for the proof of the theorem which we announced in the introduction.

The construction of the mantilla comes from a tentative implementation of Robinson's tiles in the hyperbolic plane.

Remember that Robinson's tiles for his proof of the undecidability of the general tiling problem in the Euclidean plane have the following aspect.

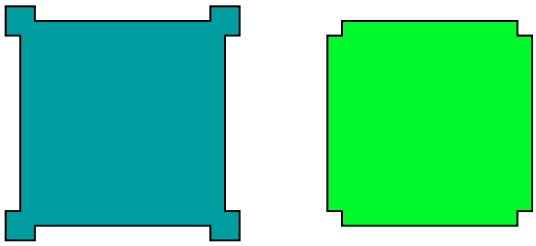

FIGURE 2. Basic patterns of Robinson's tiles for the proof of the undecidability of the general tiling problem in the Euclidean plane.

The next picture indicates a possible attempt to transport these patterns to the heptagrid. In fact, the direct translation of the patterns of Figure 2 are the

patterns (i) and (ii) of Figure 3. It is not difficult to see that these patterns cannot tile the hyperbolic plane. It is plain that the tile (ii) requires only tiles (i) around itself. However, trying to put seven copies of (i) around (ii), we are faced with a contradiction. Now, the contradiction is removed if we replace (ii) by (iii).

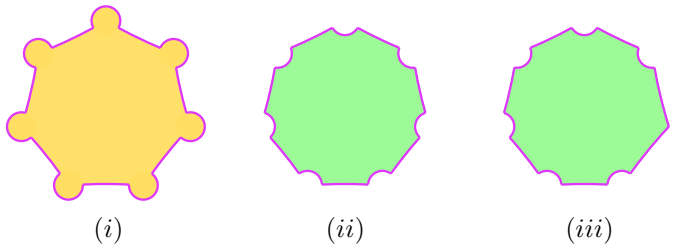

FIGURE 3. Transporting Robinson's patterns into the ternary heptagrid.

Now, we would like to replace the patterns (i) and (iii) of Figure 3 by true *à la Wang* tiles. This is not very difficult to achieve. Figure 4 gives a possible solution.

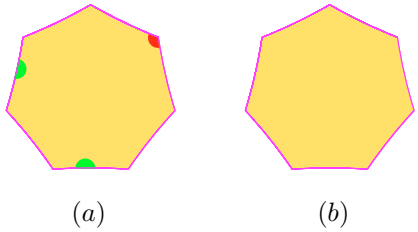

FIGURE 4. Translation of the tiles (i) and (iii) of figure 3 into true domino patterns.

This time, it is possible to assemble the tiles (a) and (b) in order to tile the hyperbolic plane. However, now there is much more freedom than in the Euclidean plane where Robinson's tiles can be assembled in a unique way.

1.3. The flowers

It is immediate to see that seven tiles (a) can be put around a tile (b). But it is possible to tile the whole hyperbolic plane with the tile (b) only. To prevent this, we put colours, which we represent by numbers in [1...7], on the edges of the tiles (b). We put the numbers in [1...7], starting from an edge with 1 and going on counter-clockwise. With this numbering of the sides, it is no more possible to tile the hyperbolic plane with the tiles (b) alone. This is due to the angle $\frac{2\pi}{3}$, as 3 is odd. Note that if we take copies of the tile (b) with the numbering in the reverse

order, it is still no more possible to tile the hyperbolic plane with the tiles (b) only, even when some of them are numbered clockwise and the others counter-clockwise.

Now, the numbers on the tile (b) induce several types of tiles (a) as they each one receive at least one number in $[1...7]$.

From now on, call **petals** the tiles of type (a) and **centres**, the tiles of type (b). We call **flower**, the figure obtained by assembling seven petals around a centre. Note that a flowers represents a ball of radius 1 around its centre.

Now, it is not difficult to see that we have several kinds of flowers.

As an example, if we fix the numbering, we have the following possibilities.

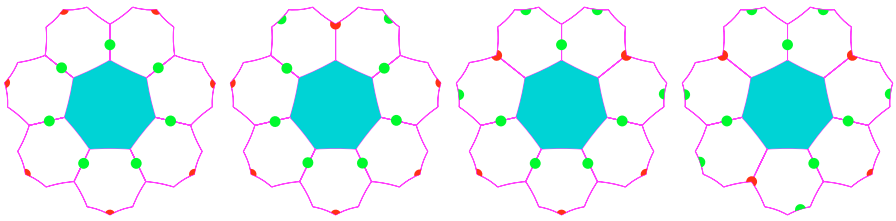

FIGURE 5. Possible types of flowers. They are ordered according to the number of flowers which can be put around them, contiguously.

As proved in [8] and also in [5], balls of radius 1 tile the hyperbolic plane. Note that petals always abut with three centres. This means that in our setting, flowers **merge**. And so, we are interested in looking at possible ways to tile the hyperbolic plane with flowers, while merging them in the way induced by the structure of the petals.

It is not difficult to see that it is not possible to tile the hyperbolic plane with 7-flowers only. The same is true for 8-flowers only and also for 10-flowers only. I don't know whether the same also holds with 9-flowers only. The situation is more difficult as there are two types of 9-flowers as will soon be seen. However, we shall see that the tiling property holds if we allow to mix 9- and 8-flowers. We shall do this in the next section.

Figure 6 illustrates the flowers which we shall keep in the rest of the paper.

We just remark that the difference between **7**-, **8**-, **9**- and **10**-flowers is defined by the number of red vertices which are directly at the distance of one edge from the centre, we shall stay at **distance 1** from the centre. It is 0, 1, 2 and 3 respectively. This classification allows us to note that for **9**-flowers, we have two cases, depending on the smallest number of petals which can be put around the centre between two red vertices at distance 1. This smallest number can be 2 or 3 defining 9f- and 9g-flowers respectively. The corresponding petals define the **upper part** of the flower. The other petals belong to its **lower part** which we also call the **non-parental** petals.

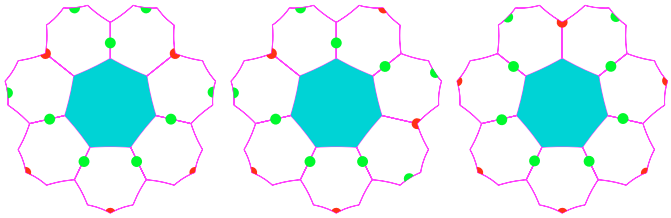

$(9f)$ $(9g)$ (8)

FIGURE 6. The flowers of the mantilla : from the left to the right, **F-flowers**, **G-flowers**, both **9**-flowers, and the **8-flowers**.

In the next sub-section, we look at the splitting of the tiling $\{7, 3\}$ into flowers which are copies of those which we have selected. The resulting tiling in terms of flowers is the **mantilla**. Later, in Section 1.5, we look at a set of tiles which forces the construction of the mantilla.

1.4. Splitting the mantilla

We start with a $9f$-flower which, from now on, we call F-flower. The leftmost picture of Figure 7 shows us how to define a region for the splitting which we shall call a **sector**. It is defined by taking the center and all the tiles delimited by this centre and the rays which start from the red vertices which are at distance 1 from the centre and which share an edge with a non-parental petal of the flower.

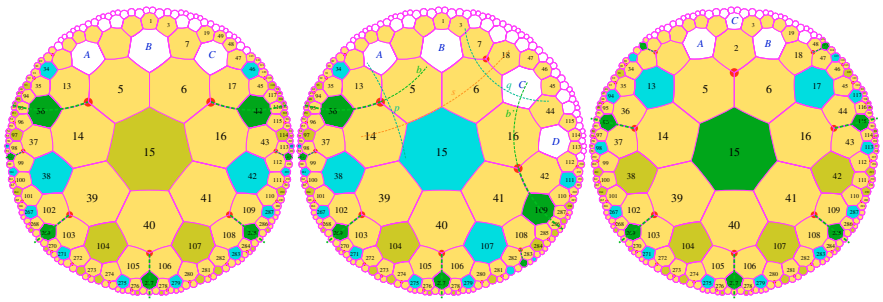

$(9f)$ $(9g)$ (8)

FIGURE 7. Splitting the sector associated to each kind of flower of the mantilla.

In the case of an $9g$-flower, which we call a G-flower from now on, we proceed to the splitting in the same way: the sector is defined by the rays issued from the red vertices, at distance 1 from the centre and by the non-parental tiles.

Looking at the leftmost picture of Figure 7, we can see that the sector of an F-flower **F** can be split into two similar sectors, associated to two F-flowers which we can define as the sons of **F**. On each side of the sons of **F**, we have a sector

defined by a G-flower which we can also consider as a son of **F**. On each side of the sector, what remains is something which contains the half of an **8**-flower.

We can formulate a similar conclusion for the sector of a G-flower. This time, the centre has a single F-son and two G-sons, one of them on each side of the F-son. As in the case of an F-centre, there is a remaining part which splits into two halves of an **8**-flower.

At last, looking at an **8**-flower, the rightmost picture of Figure 7, we define the sector of an **8**-flower as the centre of the flower together with the four sectors defined by its four F-sons.

Accordingly, arguing by induction on the number of flower we use, we can easily prove the following result:

Lemma 1.1. *The hyperbolic plane can be tiled by using copies of* **8***-, F- and G-flowers, according to the rules induced from Figure* 7*. There are uncountably many solutions.*

1.5. Tiles for the mantilla

Now, we wish to devise a finite set of tiles which **forces** the construction of the mantilla. In fact, we shall manage things in such a way that although the set of tiles will force the construction of the mantilla, it will allow all the possible solutions.

To this purpose, we fix the numbering of the centres as follows: F- and **8**-centres are numbered clockwise. Moreover, the edge **1** will be above the right-hand side red vertex at distance 1 from the centre in an F-flower, on the right-hand side of the single red vertex at distance 1 from the centre in an **8**-flower.

For G-flowers, we shall number their centres counter-clockwise. Now, for a reason which will later be clear, we distinguish two kinds of G-flowers: those which are on the right-hand side of an F- or a G-sector, and those which are on the left-hand side. They are respectively denoted G_ℓ and G_r, because the *father* of the considered G-centre is on the opposite side with respect to the side of the sector in which the considered G-centre stands. Now, in both cases, we define the edges **1** and **7** of a G-centre **G** as the edges which share a common vertex with the edge of the tiling which connects **G** with the F-centre of its father. Now, in all cases, we define the **parental petals** of a flower as its petals which share the edges **1** and **7** with the centre of the flower. It is easy to see that the parental petals of an F-flower constitute its upper part, that those of an **8**-flower share the red vertex at distance 1 from the centre and that those of a G-flower are both in contact with the G-centre and with the father of the flower.

At last, to reinforce the connection between the tiles, we append barred numbers according to the following rules: even numbers in an **8**-centre, the numbers **3**, **4** and **5** in an F-centre, the numbers **5** and **6** in a G_ℓ-centre and the numbers **2** and **3** in a G_r-centre. In a given centre, the numbers which are not indicated by the just formulated rules are not barred.

This numbering of the centres induces a numbering of the petals which is unique. Moreover, in many cases, the petal induces the centre. But this is not always

TABLE 1. Table of the non-parental petals according to their parent flower.

	2	$\overline{2}$	3	$\overline{3}$	4	$\overline{4}$	5	$\overline{5}$	6	$\overline{6}$
F	2∘77			1∘1$\overline{3}$		1$\overline{4}$7∘		$\overline{5}$7∘7	11∘6	
G_ℓ	11∘2		37∘7		1∘14			$\overline{5}$∘77		$\overline{66}$7∘
G_r		1$\overline{22}$∘		11∘$\overline{3}$	47∘7		1∘15		6∘77	
8		1$\overline{22}$∘	137∘			1$\overline{4}$7∘	157∘			$\overline{66}$7∘

the case. Now, the parental petals also define the centre. Accordingly, the set of tiles induces a tiling which observes the rules defined by Figure 7. However, there are uncountably many solutions, their cardinality being that of the continuum.

The tiles can be defined by Table 1. In the table, the petals are described by a formula of the form $\alpha\beta\gamma\delta$, where one symbol is ∘ and denotes the red vertex of the petal. The other symbols are numbers, possibly barred. The formula starts with the smallest possible number and the others follow by clockwise turning around the petal. This fixes the red vertex with respect to the numbered sides.

We refer the reader to [4] for the details of the proof. We also mention that several tables given in [4], especially the tables giving the possible couples of parental tiles for all kind of centres, can be deduced from Table 1 by a kind of reverse computation.

From this, we obtain the following result:

Lemma 1.2. *There is a set of* 21 *prototiles which forces the construction of the mantilla.*

2. The harp

In this section, we describe the implementation of a space-time diagram of the execution of a Turing machine.

We show how this implementation can be performed within a Fibonacci tree defined by an angular sector, as introduced in Section 1.1.

In the Fibonacci tree, we introduce a new splitting of the sector. Define a **black** Fibonacci tree as what we obtain by considering a tree rooted at a black node. We can obtain the usual Fibonacci trees as a disjoint union of black Fibonacci trees, applying the splitting suggested by the left-hand side picture of Figure 8. Indeed, the first black tree is rooted at the tile **1**, the root of the standard Fibonacci tree. Now, if we look at the complement of the black tree in the standard Fibonacci tree, we get an angular sector defined by the tile **4**. And so, what we just have done for the angular sector at the tile **1** can be repeated for the tile **4**: we define a black Fibonacci tree rooted at the tile **4** and, what remains in the angular sector at the tile **4** is again a standard Fibonacci tree rooted at the tile **12**. The sequence is defined by the tiles with the numbers 1, 4, 12, ..., $f_{2n+2}-1$, ..., for non-negative n.

They constitute the right-hand side border of the standard Fibonacci tree rooted at the tile **1**.

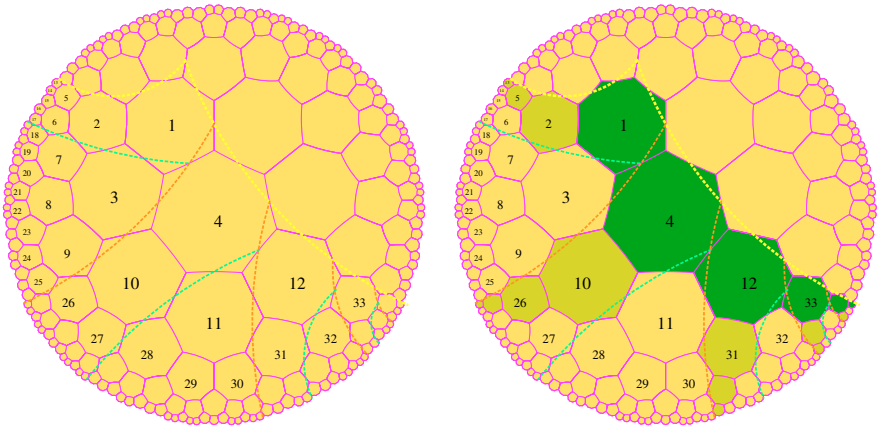

FIGURE 8. The implementation of the space-time diagram. On the left-hand side, the stack of black trees. On the right-hand side, the implementation of the chords.

Now, the chords are simply defined as the leftmost branch of each black Fibonacci tree which we have just defined. The tiles of the rightmost branch of the standard Fibonacci tree rooted at the tile **1** are the squares of the semi-infinite tape of the Turing machine whose execution is simulated by the tiling restricted to the Fibonacci tree. Each chord represents the evolution in time of the content of the considered square.

The computing works as follows.

It starts from the tile **1** and it goes to the tile **4** through the tile **3**. The tile **4** is the next tile visited by the simulated Turing machine M, as M is assumed to work on a semi-infinite tape which is initially empty. The computing signal contains the current state of the machine head and the direction of the move it has to perform. Next, each time the computing signals meets a chord, it knows the current content of the square, represented by the chord. And so, the execution of the instruction can be performed: the content of the square is changed and the signal takes the new state. Now, the computing signal performs the required move. If the move implies no change in the direction of the motion of the machine, the signal goes on on the same level, until it meets the next chord. If it is already at the end of the level or if it has to change the direction, the signal goes down by two steps along the chord with the new information and, when it is on the new level of the tree, it goes on the required direction to the nearest chord. Remind that a level of the tree consists of the tiles which are inside the tree and which are at the same distance from its root.

Now, the computing signal halts if and only if M halts. If the computing signal halts, it is not difficult to provide tiles which block the continuation of the tiling process. See [4] and Figure 14 for an implementation of a halting instruction.

The tiles to implement the motion of such a signal are not difficult to devise, see [4] for a possible implementation.

Note that this construction gives an easy proof of the undecidability of the origin-constrained problem for the hyperbolic plane. Remember that this theorem was first established in 1978 by Robinson, see [10].

3. The proof

Now, we have almost all ingredients needed for the proof. We have to see where we can place the computing areas which we have defined in Section 2. Then, we shall give some account on the set of tiles which will generate this positionment.

3.1. Threads and ultra-threads

To this purpose, we remark the following property. Take as a root of standard Fibonacci tree the centre of an F-flower F. Assume that the rays which define the tree meet on the mid-point of the edge which is shared by the parental tiles of F. Then, it is not difficult to see that the whole tree is contained in the sector defined by F. In fact, the borders of the tree do not meet the borders of the sector.

From the splitting of the mantilla by the flowers and their sectors, the just remarked property also holds for trees which would be defined inside the tree rooted at F. It is enough that the new trees are defined at an F-centre in the same way as the tree defined at F.

Let us define the **trees of the mantilla** as standard Fibonacci trees rooted at an F-son of a G-flower.

From what we have previously remarked, it is not difficult to prove the following property.

Lemma 3.1. *Consider T_1 and T_2 two trees of the mantilla. Let $sect(T_i)$ define the angular sector defined by T_i, $i \in \{1, 2\}$. Then, either $sect(T_1) \cap sect(T_2) = \emptyset$, or $sect(T_1) \subset sect(T_2)$ or $sect(T_2) \subset sect(T_1)$.*

Note that, in the statement of the lemma, the indicated inclusions are strict when they are realized.

This clearly follows from the fact that, as already noticed, the borders of a tree do not meet the borders of the sector defined by the root of the trees. As a consequence, the borders of two trees of the mantilla do not meet, which is enough to entail the lemma.

From Lemma 3.1, we define the notion of **thread** as follows: it is a set $\mathcal{F}$ of trees of the mantilla such that:

(i) if $T_1, T_2 \in \mathcal{F}$, then either $sect(T_1) \subset sect(T_2)$ or $sect(T_2) \subset sect(T_1)$;
(ii) if $T \in \mathcal{F}$, then there is $B \in \mathcal{F}$ with $sect(B) \subset sect(T)$;

(iii) if $T_1, T_2 \in \mathcal{F}$ with $sect(T_1) \subset sect(T_2)$ and if T is a tree of the mantilla with $sect(T_1) \subset sect(T)$ and $sect(T) \subset sect(T_2)$, then $T \in \mathcal{F}$,

here the indicated inclusions are strict.

Now, we say that a thread is an **ultra-thread** if it has no maximum with respect to the inclusion. It is not difficult to see that, as shown in [4], when there is an ultra-thread, it is indexed by $\mathbb{Z}$. Also, the union of the angular sectors belonging to an ultra-thread is the hyperbolic plane. From this, we can see that an ultra-thread defines a unique direction in the following sense: if $\mathcal{U}_1$ and $\mathcal{U}_2$ are ultra-threads, there is an index n_1 for $\mathcal{U}_1$ and an index n_2 for $\mathcal{U}_2$ such that the corresponding trees are identical. Accordingly, the same property holds for the trees indexed by n_i+k, with $i \in \{1, 2\}$ and positive k.

It is not difficult to see that there may be realizations of the mantilla with an ultra-thread. There are also realizations without ultra-thread.

3.2. The computing areas

For our computation, we consider a realization of the mantilla without ultra-thread. This means that each thread has a maximal element which is in fact a maximum. We select this element $\mathcal{M}$ and we decide that the F-sons of a G-flower which are inside $sect(\mathcal{M})$ do not generate a tree of the mantilla. In the next sub-section, we shall see that this condition is easy to be realized with a set of tiles.

The implementation of the trees of the mantilla is indicated by the left-hand side picture of Figure 9.

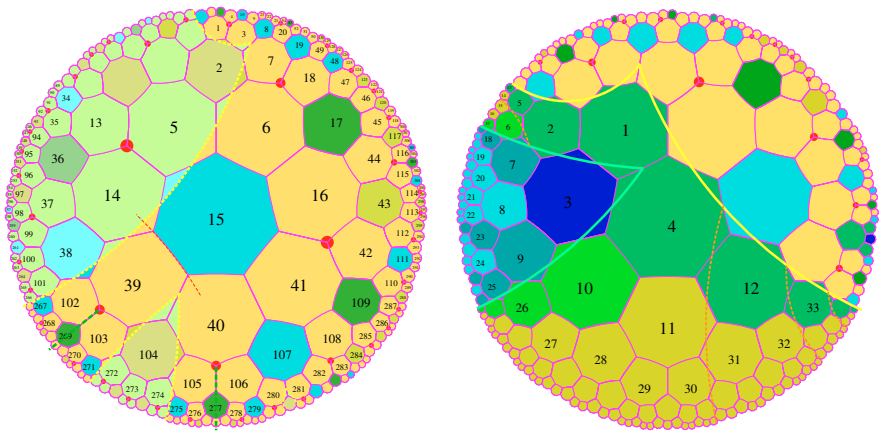

FIGURE 9. The implementation of the computing areas in the mantilla. On the left-hand side: the definition of the trees of the mantilla. On the right-hand side: the organization of the computing area inside a tree of the mantilla.

The right-hand side picture of the figure indicates the implementation of the harp within a selected tree of the mantilla.

As can be seen from the right-hand side picture, the harp is not identical with a tree of the mantilla, as delimited in the left-hand side figure. The harp is a sub-tree of a tree of the mantilla whose angular sector is strictly embedded in that of the tree of the mantilla. The reason is that the tiles used for the harp may have computing marks. If such a tile is taken randomly, it may introduce a perturbation, whatever the computation of the Turing machine M. In fact, the tiling must force a beginning of the computation at the root of the harp which plays the rôle of an origin. This is why we introduce a **shield** between the harp and the tree of the mantilla which contains it. The shield forces the tiling to append tiles until an origin occurs. It may happen that such an origin is never found. But in this case, we have a half-plane where no computation happens but in the complementary half-plane, infinitely many computations happen.

3.3. The tiles

Now, let us turn to the set of tiles.

In fact, we have three categories of tiles:

(i) the tiles for the mantilla itself;
(ii) the tiles for the shields;
(iii) the tiles for the harp.

The connection between the three groups of tiles is performed by the F-sons of a G-flower which give rise to a tree of the mantilla.

Figure 10 displays the tiles for the mantilla itself. The last three rows of the figure indicate the tiles which are at the border of a shield raised by and F-son of a G-flower.

Figures 11 and 12 display the tiles for the shield. In Figure 11, we have the tile for the root and the tiles which are inside the shield. Note that the tiles on the first row of Figure 11 bear signs of the harp.

In Figure 12, we have the tiles of the shield which belong to the border of the shield with the mantilla: on the first row, the tiles concerned by the left-hand side border and, on the second row, those which belong to the right-hand side border.

Figures 13 and 14 give the tiles for the harp. In Figure 13, we have the tiles of the harp which are on the border with the shield.

It is the point to note, here, that the tiles of the mantilla are no more involved in the shield and in the harp. In these domains of a computing area, the background of the tiling consists of patterns which simply propagate the structure of a Fibonacci tree. This is performed by the tiles `black` and `white` in Figure 11 for the shield and by the two tiles labeled `background` in Figure 14.

Figure 14 bears the computing signals. We can see those which correspond to the content of a square of the tape, labeled `cell` and `right`, without state signal, those with the computing signal, labeled `state`, and those which perform an instruction, labeled `trans.`, `cont.` and `halt`. Note the two tiles associated with the transfer to the halting state which block the construction of the tiling.

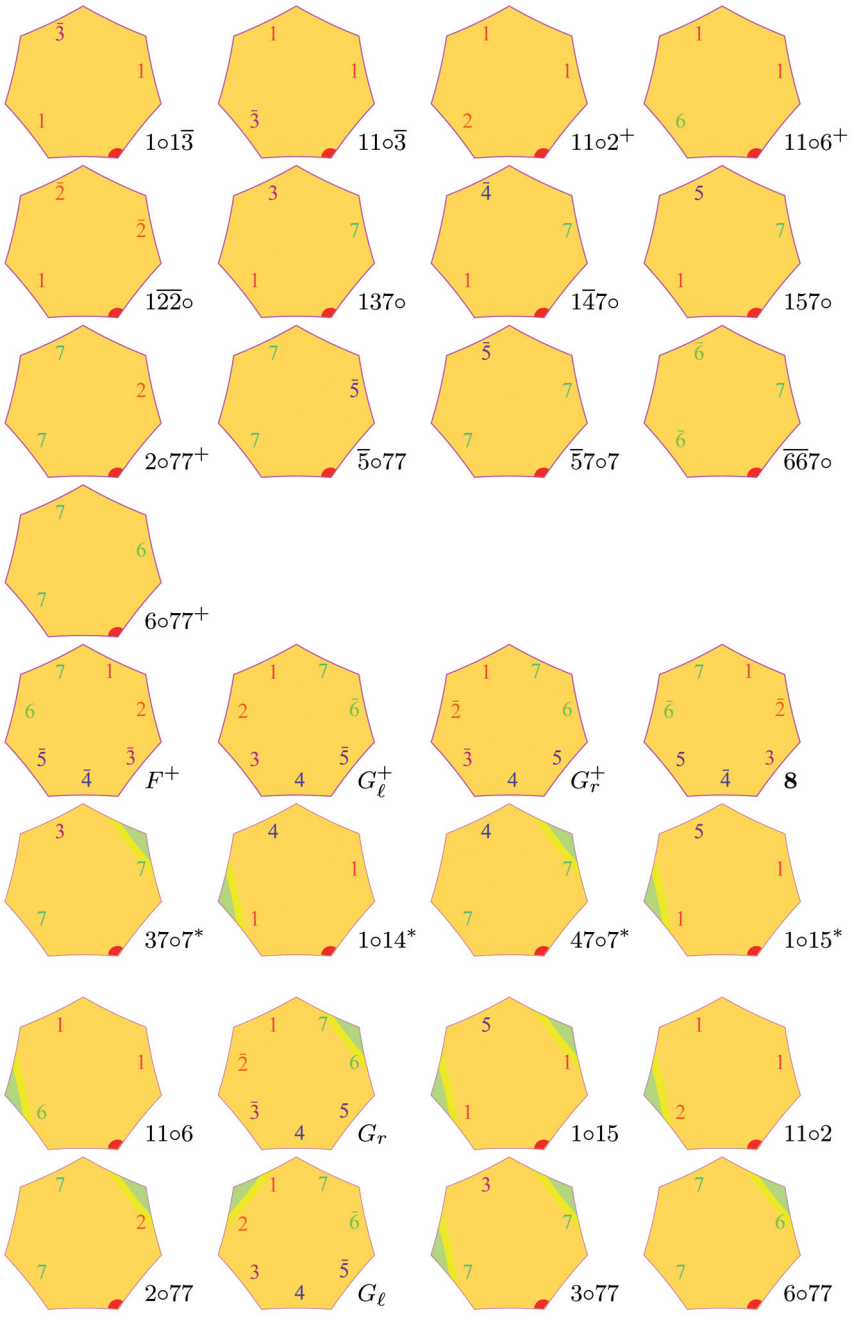

FIGURE 10. The 29 tiles of the mantilla and the implementation of its trees. Note the tiles which start the construction of a selected tree.

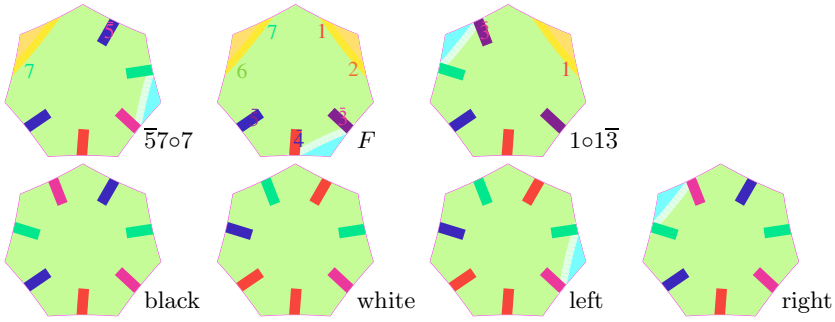

FIGURE 11. Tiles of the shield. Note the two tiles of the shield which are on the border of the harp.

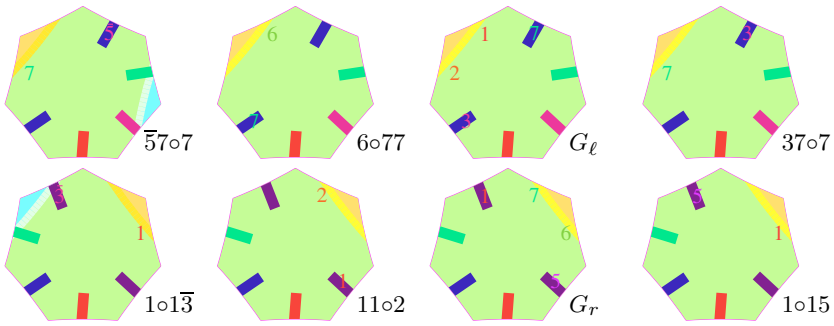

FIGURE 12. The other tiles of the shield. First row: the 4 tiles of the shield which belong to the border between the mantilla and the left-hand part of the shield. Second row: the 4 tiles of the shield which belong to the right-hand part of the shield.

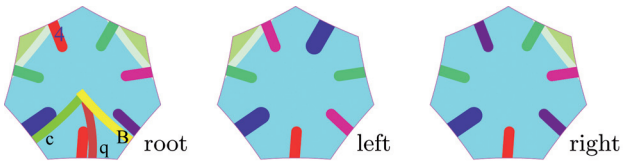

FIGURE 13. The tiles of the borders between the shield and the harp. Note that the marks of the mantilla disappeared on the two right-hand side tiles.

They bear black numbers which can abut with themselves only. Now, the patterns of the tiles make it impossible to turn them or to reflect them in a symmetry axis. And so, if such a tile is put on the tiling, the construction is blocked.

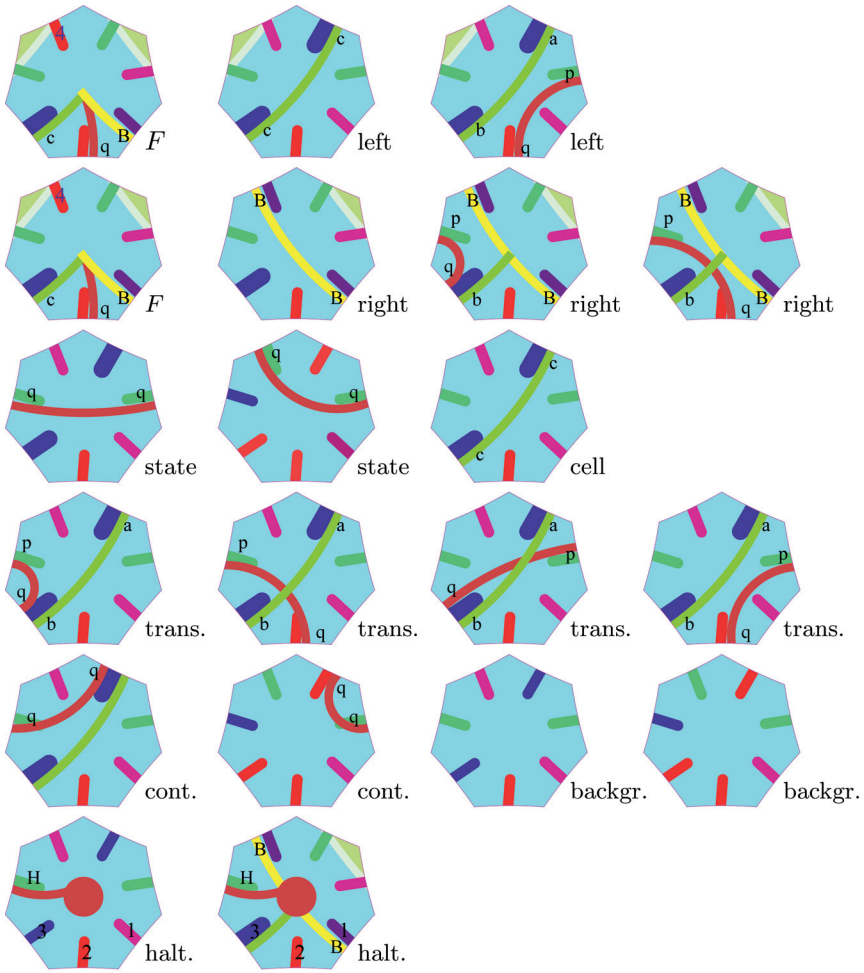

FIGURE 14. The tiles for the harp and its computation.

3.4. THE PROOF

Now, the proof of the properties defining the generalized origin-constrained problem is easy. Figure 8 shows that in a ball of radius 6 around an F-son of a G-flower giving rise to a computing region, *i.e.* an origin ω, there are two origins: each one on each side of the computing area defined by ω. It is plain that ω does not belong to the line defined by these two origins. Now, this argument can be repeated with each origin. If we always consider the right-hand side origin, we get a ray, as the configuration is periodically repeated by the shift which joins an origin to the next one.

Now, on each origin, we can take the origin which is not on the ray which we have just defined. In this way, it is easy to construct infinitely many rays containing infinitely many origins.

Accordingly we proved:

Theorem 3.2. *The generalized origin-constrained tiling problem is undecidable in the hyperbolic plane.*

Conclusion

At the moment of writing this paper, I have a proof of the undecidability of the unconstrained tiling problem in the hyperbolic plane. However, this proof has only been partially checked by another person than the author and it is presently under refereeing. The proof was deposited on `arXiv`, see [6] and a short account of it, also submitted, was recently deposited on `arXiv`, see [7].

Acknowledgements. I wish to thank again Serge Grigorieff for his attention to this work. In the same line, I have to thank very much Tero Harju.

References

[1] R. Berger, The undecidability of the domino problem. *Mem. Amer. Math. Soc.* **66** (1966) 1–72.

[2] Ch. Goodman-Strauss, A strongly aperiodic set of tiles in the hyperbolic plane. *Invent. Math.* **159** (2005) 119–132.

[3] M. Margenstern, New tools for cellular automata of the hyperbolic plane. *J. Univ. Comput. Sci.* **6** (2000) 1226–1252.

[4] M. Margenstern, About the domino problem in the hyperbolic plane from an algorithmic point of view, *Technical report,* 2006–101*, LITA, Université Paul Verlaine − Metz* (2006), available at: `http://www.lita.sciences.univ-metz.fr/~margens/hyp_dominoes.ps.gzip`

[5] M. Margenstern, Fibonacci numbers and words in tilings of the hyperbolic plane. *TUCS Gen. Publ.* **43** (2007) 36–41.

[6] M. Margenstern, About the domino problem in the hyperbolic plane, a new solution, `arXiv:cs.CG/0701096` (2007).

[7] M. Margenstern, The domino problem of the hyperbolic plane is undecidable, `arXiv:0706.4161` (2007).

[8] M. Margenstern, *Cellular Automata in Hyperbolic Spaces*, Volume 1, *Theory.* OCP, Philadelphia (2007).

[9] R.M. Robinson, Undecidability and nonperiodicity for tilings of the plane. *Invent. Math.* **12** (1971) 177–209.

[10] R.M. Robinson, Undecidable tiling problems in the hyperbolic plane. *Invent. Math.* **44** (1978) 259–264.

[11] H. Wang, Proving theorems by pattern recognition. *Bell System Tech. J.* **40** (1961) 1–41.